ASTRONOMY & ASTROPHYSICS
SUPPLEMENT SERIES

*Astron. Astrophys. Suppl. Ser.* **112,** 235-255 (1995)



# Compact steep-spectrum sources – polarisation observations at 1.6, 4.9, 8.4 and 15 GHz

Chidi E. Akujor[1,2,3,4] and S.T. Garrington[2]

[1] Onsala Space Observatory, Onsala, S-439 92, Sweden
[2] University of Manchester, Nuffield Radio Astronomy Laboratories, Jodrell Bank, Cheshire, SK11 9DL, UK
[3] School of Physical Sciences, Imo State University, Owerri, Imo State, Nigeria
[4] Max-Planck Institut fur Radioastronomie, Auf dem Hügel 69, 53121 Bonn, Germany

Received October 30, 1994; accepted February 17, 1995

**Abstract.** — We present observations of compact steep-spectrum (CSS) sources made with the VLA at several frequencies. At 8.4 GHz we have mapped all CSS sources in the 3C catalogue (except for four very small sources) at a resolution of 0.25 arcsec. We find that the fractional polarization is rather low: the median value of the individual source components is 3%. A number of sources show striking asymmetry in their polarization distribution. We have observed 18 of the larger sources at 1.5 (or 1.6) and/or 4.9 GHz with scaled arrays at 1.2 arcsec resolution. A number of sources have been observed at 15 GHz to complement previous studies.

**Key words:** polarization — galaxies: active — quasars — radio continuum: galaxies

## 1. Introduction

Compact steep-spectrum (CSS) sources are thought to be intrinsically small (Fanti et al. 1990), unlike the flat spectrum compact sources, whose small sizes and dominant cores are ascribed to the effects of projection and Doppler boosting (Orr & Browne 1982). It remains a matter of debate whether this is because the CSS sources are young, or because they are confined by their surroundings for the majority of their lifetimes (Fanti et al. 1985). Radio polarization observations offer a way to investigate the environments of these sources via the Faraday effect. The phenomenon of depolarization asymmetry in radio galaxies and quasars is now well established (Garrington et al. 1988; Laing 1988; Liu & Pooley 1991) and provides information on the distribution of the gas responsible for the depolarization.

Because of the small size of CSS sources, their polarization characteristics have not yet been studied in as much detail as the extended sources. Several CSS sources show very high integrated rotation measures (Kato et al. 1987) and early results from VLA polarization observations at 5 GHz suggest low polarization (van Breugel et al. 1984), perhaps because of denser gas surrounding the CSS sources. Ideally, one would like to map a sample of CSS sources at two or more wavelengths with similar resolutions to measure the Faraday depolarization (cf. Garrington et al. 1991).

Here we present observations of a well defined sample of CSS sources made using the VLA at 8.4 GHz and $\simeq 0.25$ arcsec resolution. This will allow comparison with VLA maps at 15 GHz and MERLIN maps at 1.6 GHz. We have extended the work of van Breugel et al. (1992) by observing a further ten sources at 15 GHz. We have also made scaled-array observations at 1.5 (or 1.6) and/or 5 GHz of 18 CSS sources with angular sizes larger than 1.5 arcsec.

## 2. Observations

### 2.1. *8.4 GHz*

We have chosen CSS sources from the 3C catalogue using criteria similar to those of Fanti et al. (1990), namely spectral index $\alpha > 0.6$, luminosity $P_{178} > 10^{25}$ WHz$^{-1}$sr$^{-1}$ and linear size $D \lesssim 15$ kpc[1]. The revised 3C sample of Laing et al. (1983) was not used because several CSS sources fall below its increased flux density limit. We have omitted a few sources (3C119, 3C258, 3C287, 3C343) which would have been completely unresolved with the VLA at 8.4 GHz and one source (3C454) could not be observed within the ST range of our observations. We also observed 3C299, which was originally classified as a CSS source, but is now known to be a very asymmetric double

[1]Linear sizes and luminosities were calculated using $H_0 = 100$ kms$^{-1}$Mpc$^{-1}$, $q_0 = 0.5$.

source 33 kpc across (Liu & Pooley 1991) and 3C293 which might be better classified as a steep-spectrum core embedded in a much larger radio galaxy (Bridle et al. 1981). We stress that the linear size cut-off is not very exact: in particular a few sources have weak emission extending to slightly larger scales.

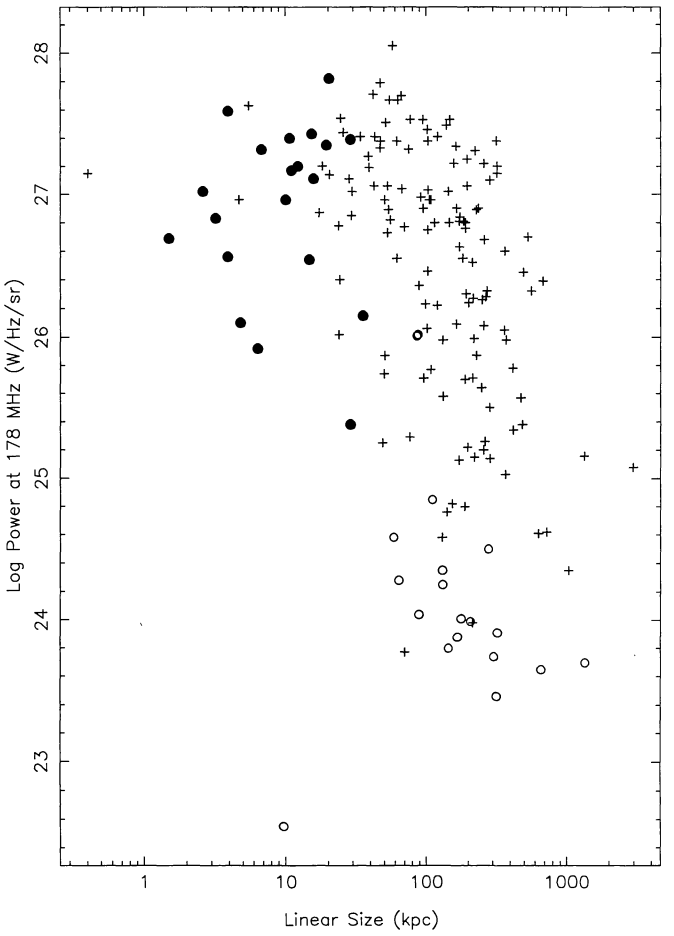


**Fig. 1.** Luminosity – size diagram for the revised 3C sample. CSS sources in the revised sample are highlighted by filled circles; crosses marked extended FR2 sources and open circles mark FR1 sources

Table 1 gives further details of the sources. Figure 1 shows where the CSS sources lie in the luminosity-size diagram for the revised 3C sample of Laing et al. (1983). (For consistency, the CSS sources in the present sample which are not included in the revised 3C sample are not included in the figure.)

The observations were made in August and September 1991 with the VLA in A or A/B configuration. A power failure during the first observing run led to the loss of all antennas along the northern arm. All sources were observed for approximately 5 minutes at the standard frequencies of 8.415 and 8.465 GHz which were later combined to give a total bandwidth of 100 MHz. Calibrator sources chosen from the VLA Calibrator List were

**Table 1.** CSS Sample

| name | $z$ | ID | las/arcsec | $D$/kpc |
|---|---|---|---|---|
| 3C43 | 1.460 | Q | 2.6 | 11.1 |
| 3C48 | 0.367 | Q | 0.4 | 1.2 |
| 3C67 | 0.310 | G | 2.6 | 7.3 |
| 3C93.1 | 0.244 | G | 0.2 | 0.6 |
| 3C138 | 0.759 | Q | 0.6 | 2.4 |
| 3C147 | 0.545 | Q | 0.3 | 1.3 |
| 3C173 | 0.292 | G | 2.5 | 6.8 |
| 3C186 | 1.063 | Q | 2.2 | 9.4 |
| 3C190 | 1.197 | Q | 2.7 | 11.6 |
| 3C191 | 1.956 | Q | 4.8 | 19.7 |
| 3C213.1 | 0.194 | G | 6.0 | 9.8 |
| 3C216 | 0.670 | Q | 2.5 | 10.0 |
| 3C237 | 0.877 | G | 1.1 | 4.6 |
| 3C241 | 1.617 | G | 0.9 | 3.8 |
| 3C266 | 1.275 | G | 4.6 | 19.8 |
| 3C268.3 | 0.371 | G | 1.4 | 4.3 |
| 3C277.1 | 0.321 | Q | 1.7 | 4.9 |
| 3C286 | 0.849 | Q | 3.3 | 13.7 |
| 3C298 | 1.439 | Q | 1.5 | 6.4 |
| 3C293 | 0.045 | G | 3.6 | 4.3 |
| 3C299 | 0.367 | G | 11.0 | 33.8 |
| 3C303.1 | 0.267 | G | 1.2 | 3.1 |
| 3C305.1 | 0.132 | G | 2.3 | 3.5 |
| 3C309.1 | 0.904 | Q | 2.0 | 8.6 |
| 3C318 | 0.752 | G | 1.0 | 4.1 |
| 3C343.1 | 0.750 | G | 0.3 | 1.2 |
| 3C346 | 0.161 | G | 13.0 | 23.4 |
| 3C380 | 0.691 | Q | 3.7 | 14.7 |
| 3C454.1 | 1.840 | G | 1.6 | 6.7 |
| 3C455 | 0.543 | G | 3.3 | 11.9 |

observed roughly once every hour for amplitude, phase and instrumental polarization calibration. Observations of 3C286 were used to set the flux density scale (Baars et al. 1977) and the polarization position angles, assuming a value of 33°. For some of the later re-observations, the calibrator observations were more scarce and so the instrumental polarization corrections were carried over from previous days. The instrumental residual polarization, after calibration, is between 0.1 and 0.5%. We have used a standard value of 0.3% throughout.

The data were calibrated, mapped and self-calibrated using AIPS on the Convex at the Onsala Space Observatory. Several cycles of phase self-calibration, deconvolution and editing were carried out for each source and a final amplitude self-calibration was used for some of the stronger sources.

### 2.2. *1.5 GHz and 5 GHz*

Sources with angular sizes larger than 1.5 arcsec were also observed at 1.5 and 5 GHz. The observations were made in A configuration at 1.3 – 1.6 GHz and in B configuration at

5 GHz in August and September 1991. This gives a common resolution of 1 − 1.2 arcsec, which is just sufficient to separate the two main components of most of these sources. The observations made without the antennae of the northern arm at 1.3/1.6 GHz were for about 8 mins each, while some sources were then reobserved with either A, or A/B array. All later observations were snap–shots typically of 5 minutes duration, some at low elevations which resulted in a non-circular beam. The calibration of the polarization position angle is less secure for some of the later re-observations where observations of 3C286 were scarce. The 5 GHz B–array observations were typically of 8 minutes duration. The mapping procedure was as described for the 8.4 GHz data.

### 2.3. *15 GHz*

A number of sources were also observed at 15 GHz in A-configuration. These observations were chosen to complement the observations by van Breugel et al. (1992) so that by combining the results we have 15 GHz data on all but 4 of the complete sample. Most of the maps required an initial self-calibration from a point-source model because the calibrator observations were insufficient to follow the tropospheric phase fluctuations. Otherwise, calibration and mapping details are as before. Our 15 GHz maps have resolutions of 120 mas.

## 3. Results

The maps are shown in Figs. 2-4, while the observational parameters are given in Tables 2-4. The polarization is represented by vectors parallel to the E-field and with lengths proportional to the fractional polarization. The contour levels, peak flux densities and polarization vector scales are given in Tables 4 and 5.

The polarization of the subcomponents of each source was measured using a vector average,

$$m_v = ((\Sigma Q)^2 + (\Sigma U)^2)^{1/2}/\Sigma I,$$

and a scalar average, $m_s = \Sigma P/\Sigma I$.

The polarized flux density maps were corrected for noise bias by subtracting the noise in quadrature. The error in the fractional polarization has been set at 0.3% unless the error due to the noise is greater in which case that has been used. Similarly, the minimum detectable polarization has been set at 0.3% or 3 times the noise error, whichever is the greater.

For the 1.6 and 4.9 GHz maps, only the vector polarization was calculated, since the individual components were barely resolved. The errors in fractional polarization are not shown since in all cases they are dominated by the residual instrumental polarization at around 0.3%.

## 4. Comments on individual sources

**3C43 (0127+23)**
The 8 GHz map shows the triple structure as seen in previously published maps (Pearson et al. 1985; Spencer et al. 1989; Akujor et al. 1991). The pattern of the magnetic field vectors follows the jet seen in high resolution maps.
**3C48 (0134+32)**
Both the 8.4 and 15 GHz maps show a decrease of the degree of polarization towards the core which is at the southern tip of the source (Wilkinson et al. 1990).
**3C67 (0221+27)**
A recent MERLIN 6 cm map (Sanghera et al. 1994) shows that there is a weak nucleus about 0.8 arcsec north of the southern component which is seen as an extension of the southern lobe in our 8 GHz map. This source shows striking polarization asymmetry at 8.4 and 5 GHz, but is unpolarized at 1.5 GHz.
**3C93.1 (0345+33)**
This source is barely resolved at 8.4 GHz.
**3C138 (0518+16)**
This source has been discussed in detail by Akujor et al. (1993). It shows a striking asymmetry in the degree of polarization at 8.4 and 15 GHz.
**3C147 (0538+49)**
The extension to the south-east of this source is highly polarized, but at this resolution the polarization in the jet is low at 8.4 and 15 GHz.
**3C173 (0658+38)**
The 8.4 and 15 GHz maps shows a central component with flux density of about 1 mJy. A faint jet leading to the eastern component is seen at 8.4 GHz. This source shows striking polarization asymmetry at 8.4 and 5 GHz, but is unpolarized at 1.5 GHz.
**3C186 (0740+38)**
The 8.4GHz map confirms the basic jet structure seen in previous maps by Cawthorne et al. (1986) and Spencer et al. (1989). Polarization is barely detected along the jet at 8.4 GHz. At 15 GHz only the core component is detected (map not shown).
**3C190 (0758+14)**
The faint extension to the south is evident in the lower resolution maps and an earlier 5 GHz map (Pearson et al. 1985). This extension is highly polarized at 8.4 GHz.
**3C191 (0802+10)**
The jet is strongly polarized but the northern component depolarizes strongly between 8.4 and 15 GHz (Kronberg et al. 1990).
**3C213.1 (0858+29)**
The low resolution maps show a large diffuse halo surrounding this source with a total extent of 40 arcsec along the source axis. At 8.4 GHz, the compact components to the north and south are highly polarized and we detect a bright, unpolarized central core.
**3C216 (0906+43)**
The jet to the south of the core (Fejes et al. 1992) is clearly

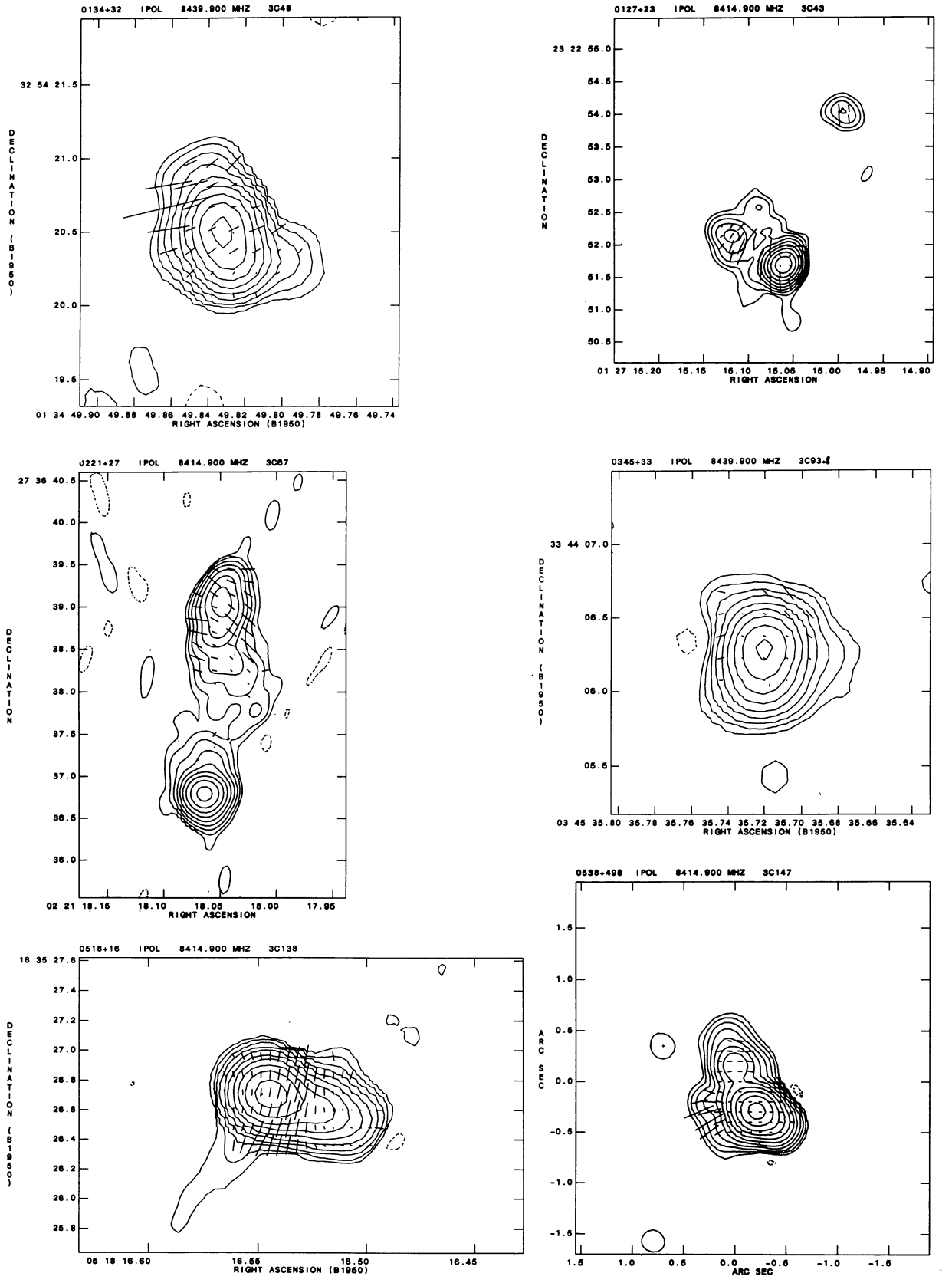


**Fig. 2.** Maps of CSS sources at 8.4 GHz. Details of the contour levels and the scale for the polarization vectors are given in Table 5

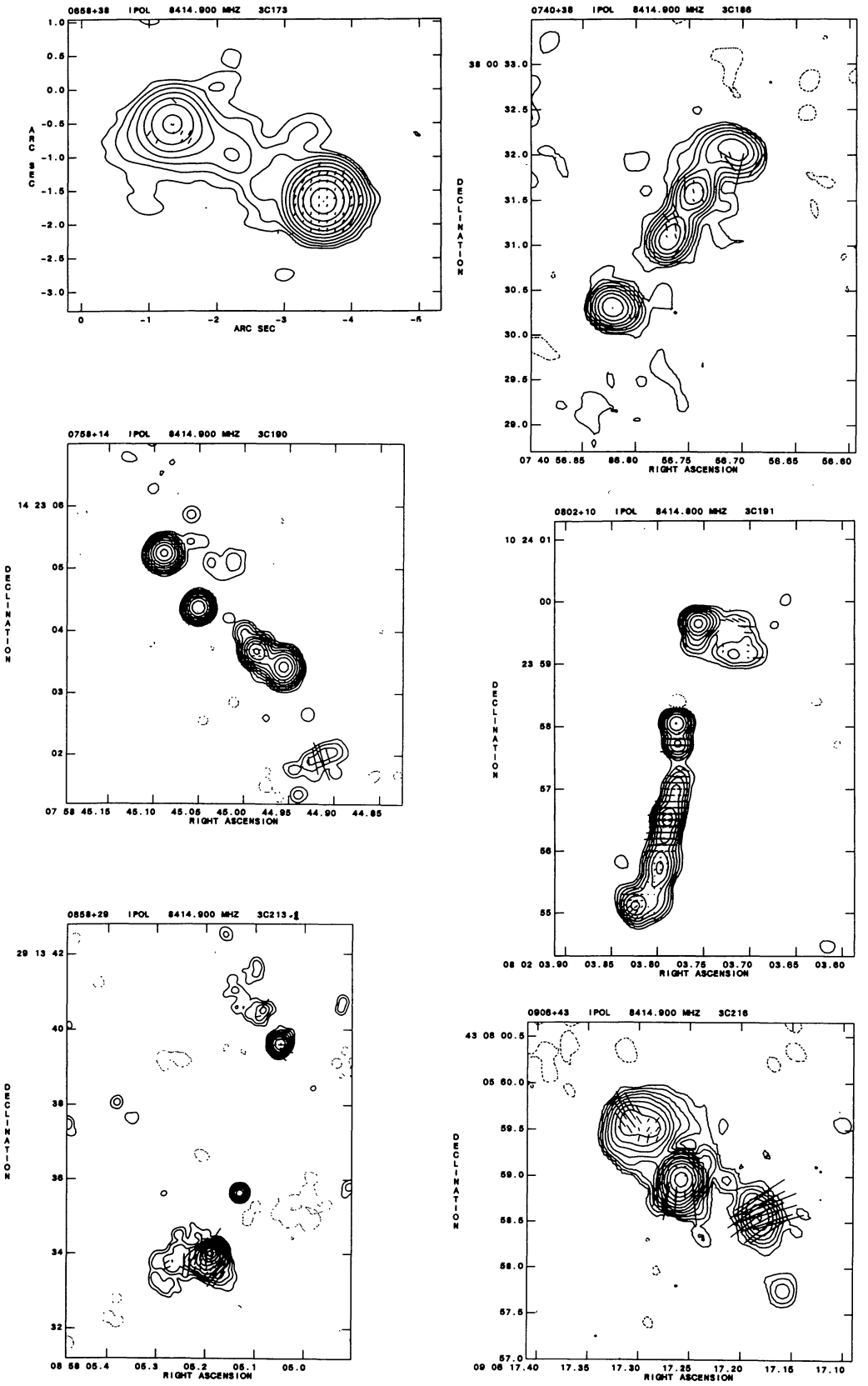


**Fig. 2.** continued

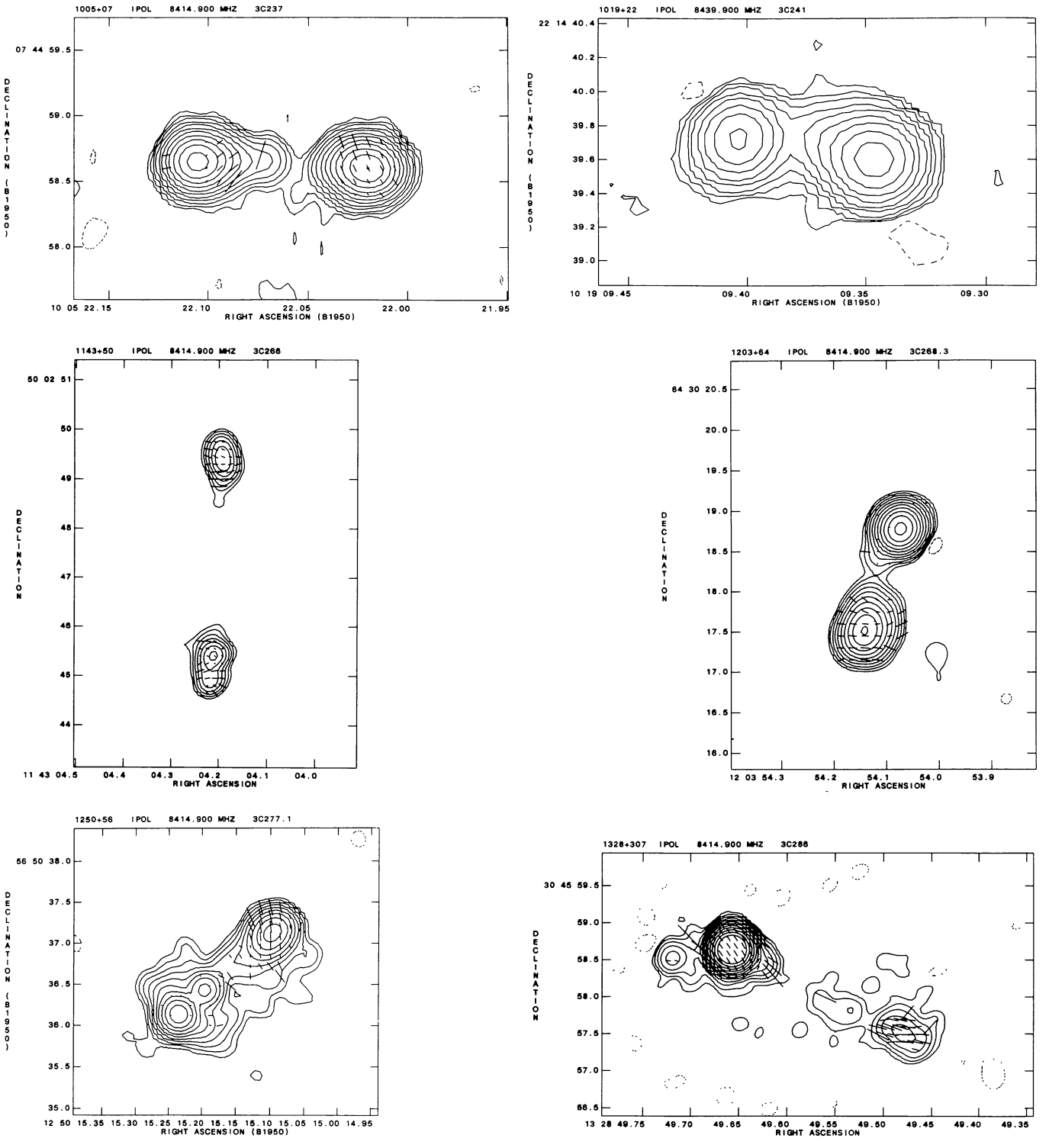


**Fig. 2.** continued

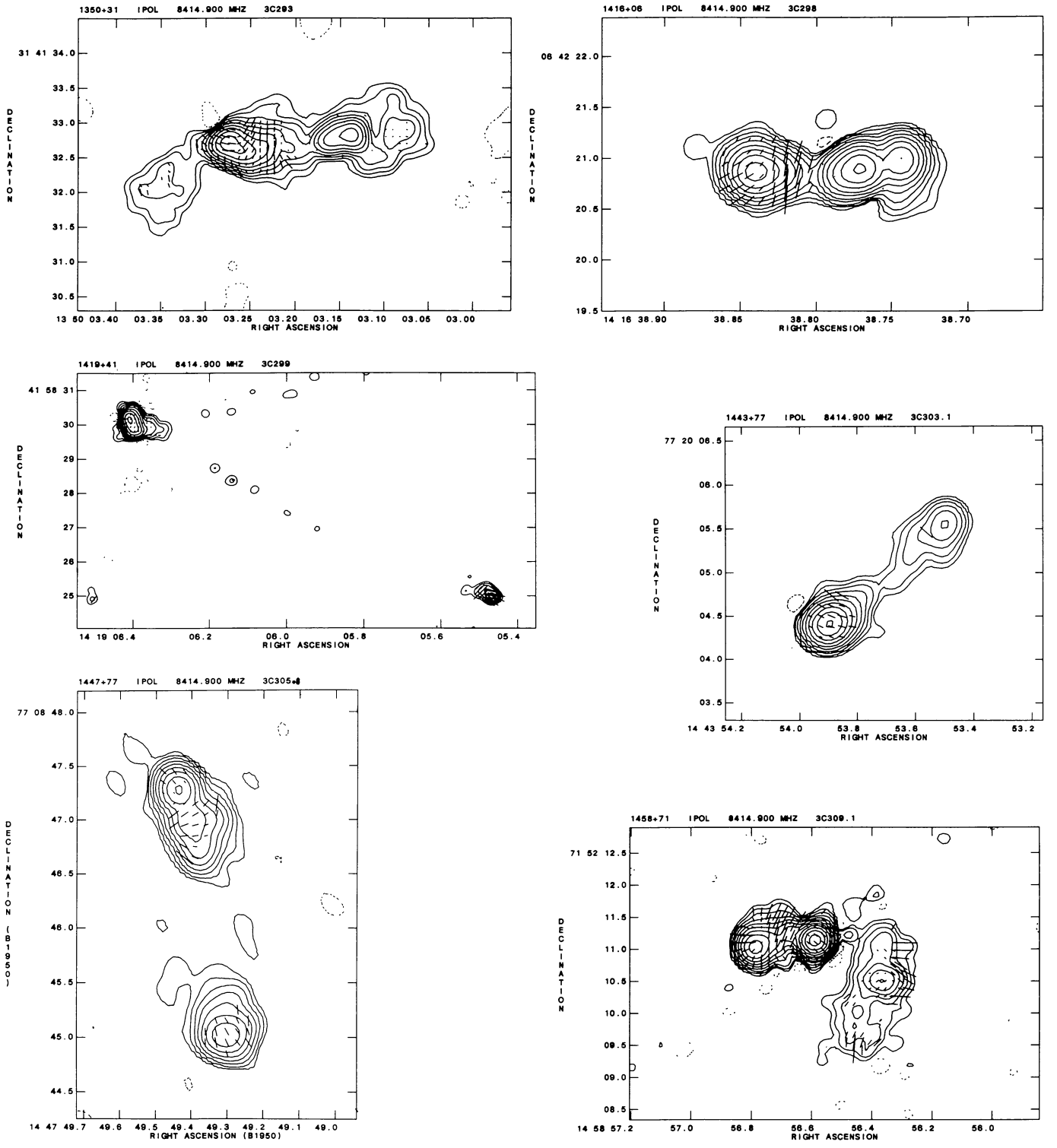


Fig. 2. continued

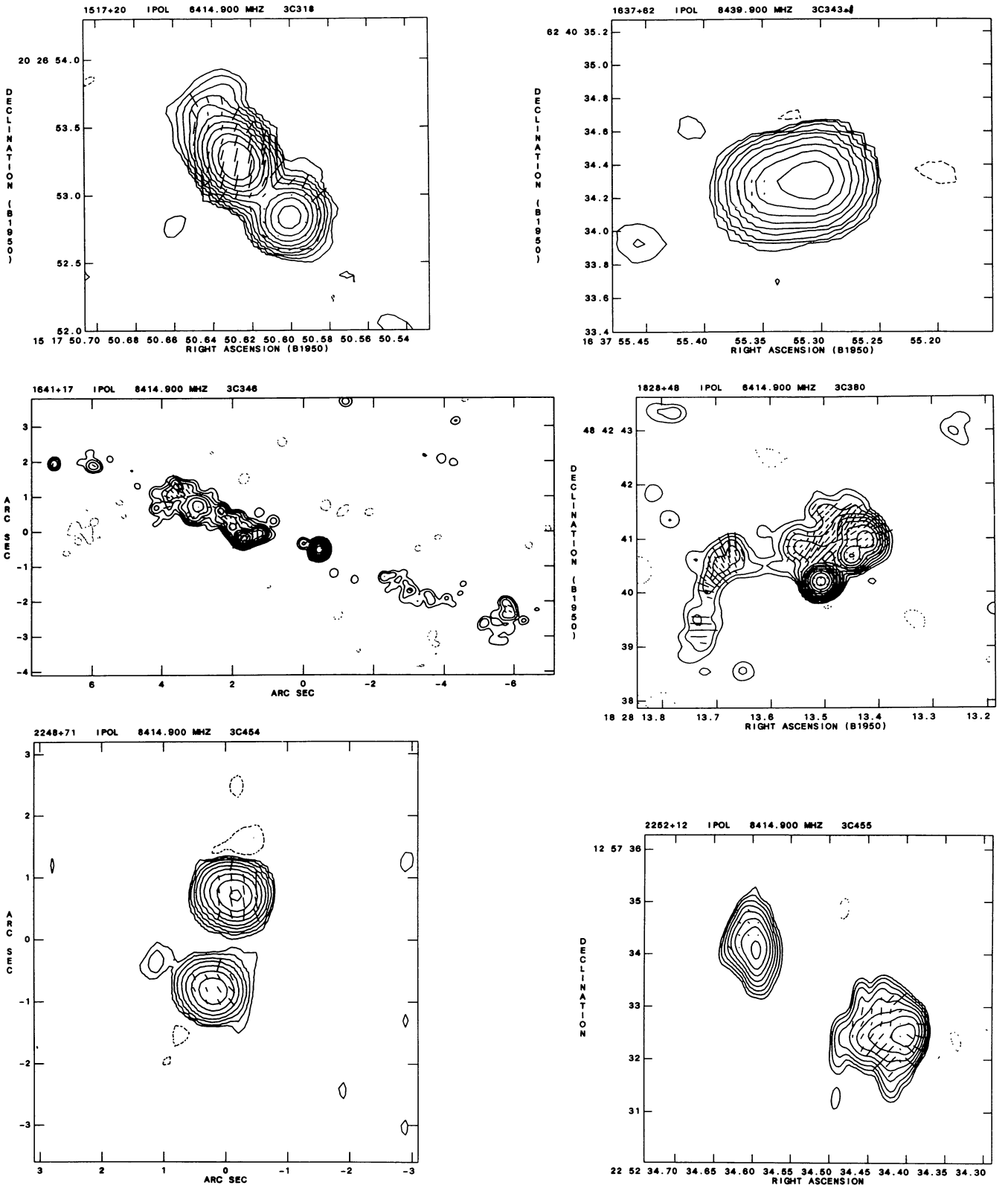


**Fig. 2.** continued

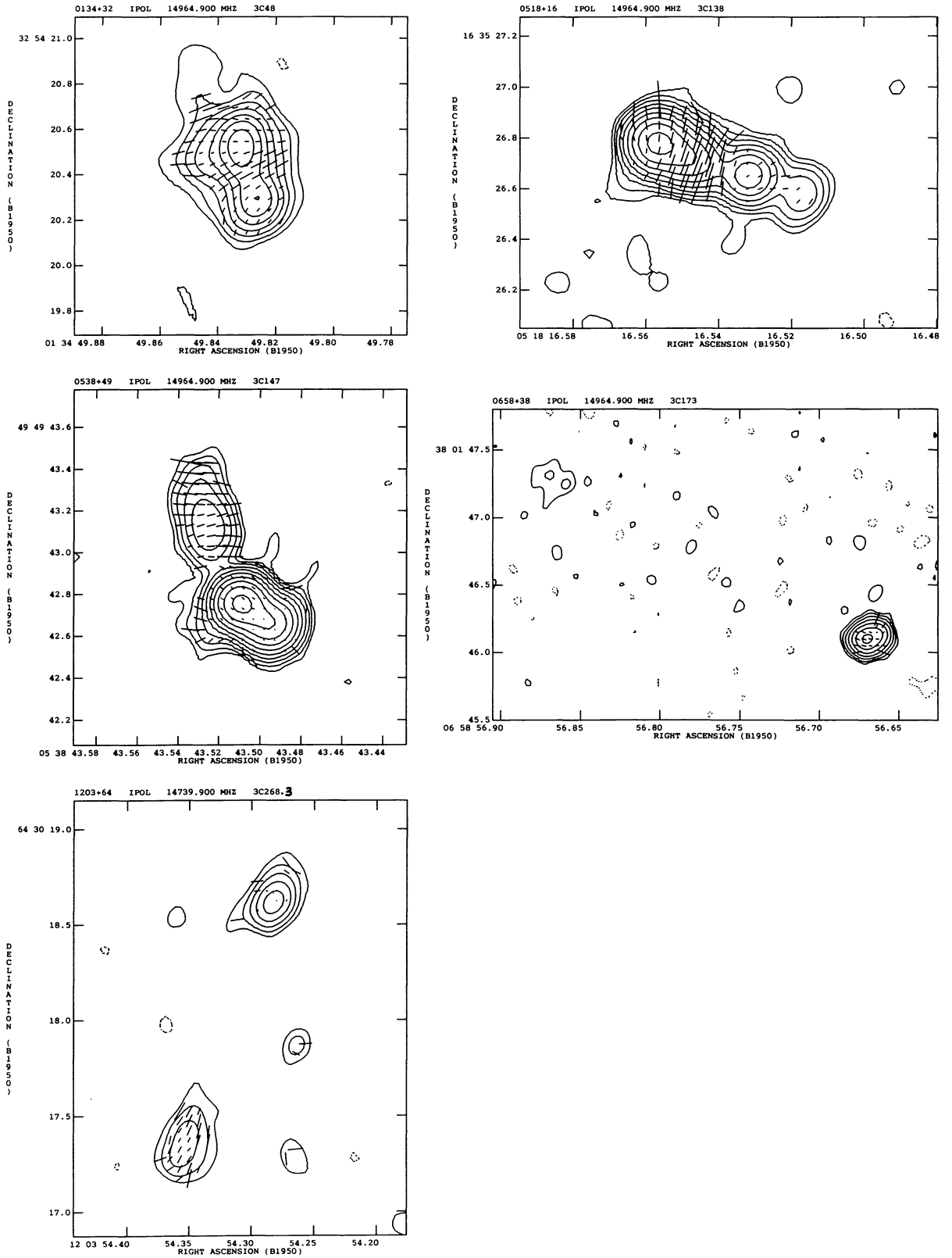


**Fig. 3.** Maps of CSS sources at 15 GHz. Details of the contour levels and the scale for the polarization vectors are given in Table 5

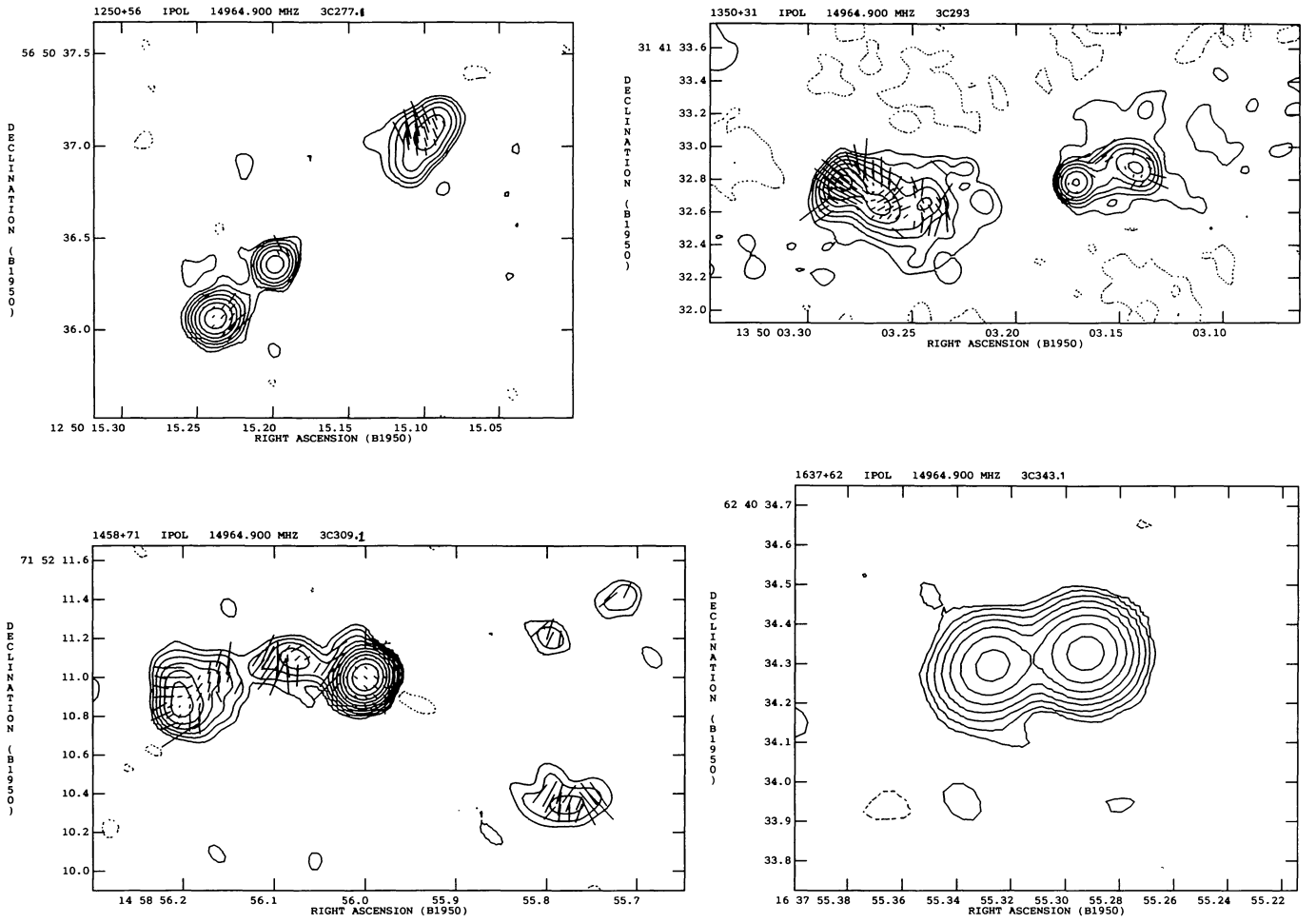


**Fig. 3.** continued

apparent as a highly polarized extension to the core in this map. This source is discussed in detail by Akujor et al. (1994, in prep.).

### 3C237 (1005+07)

The 8.4 GHz map shows a polarized region between the eastern hotspot and the core. A similar feature is seen by van Breugel et al. (1992) at 15 GHz.

### 3C241 (1019+22)

No significant polarization has been detected at 8.4 GHz or 15 GHz (van Breugel et al. 1992).

### 3C266 (1143+50)

This source is fairly symmetric in polarization at 8.4 GHz

### 3C268.3 (1203+64)

This source shows very asymmetric polarization at both 8.4 and 5 GHz (see van Breugel et al. 1984). The weak core seen in the MERLIN map by Sanghera et al. (1994) is present as an extension of the northern component of our 8.4 GHz map.

### 3C277.1 (1250+56)

This source shows a striking asymmetry in polarization at 8.4 GHz.

### 3C286 (1328+30)

The jet to the W of the core is highly polarized with **E**-vectors parallel to the jet axis at 8.4 GHz.

### 3C293 (1350+31)

This source is the steep spectrum core of a much larger radio galaxy (Bridle et al. 1981). We confirm the low brightness extensions intermediate in scale between the compact lobes and the large scale structure (Pearson et al. 1985). We identify the bright central feature in the 15 GHz map as the nucleus of this source as previously suggested by van Breugel et al. (1984)

### 3C298 (1416+06)

The 8.4 GHz map presented here and the 15 GHz map of van Breugel et al (1992) show that the jet to the east of this source is highly polarized where it joins the outer component. The two outer components show significant polarization asymmetry.

### 3C299 (1419+41)

Liu and Pooley (1991) and van Breugel et al. (1992) find a central component near to the northern component. This confirms that this source is an asymmetric double radio

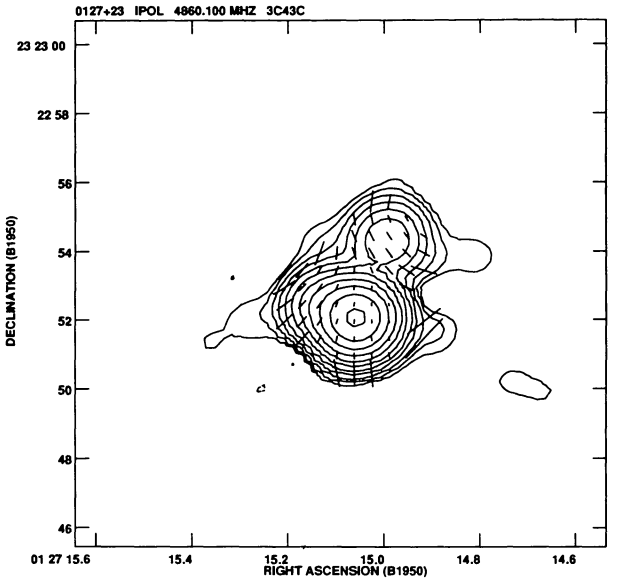


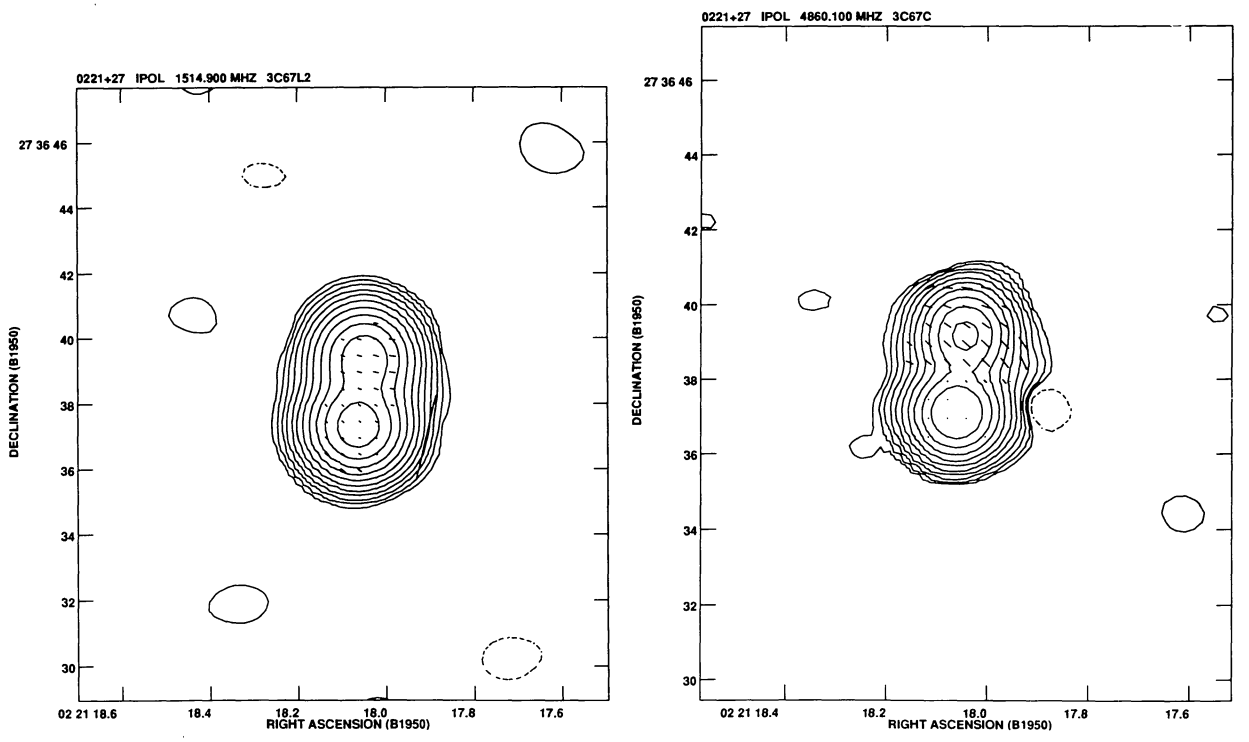


**Fig. 4.** Maps of CSS sources at 1.5 and 4.9 GHz. Details of the contour levels and the scale for the polarization vectors are given in Table 6

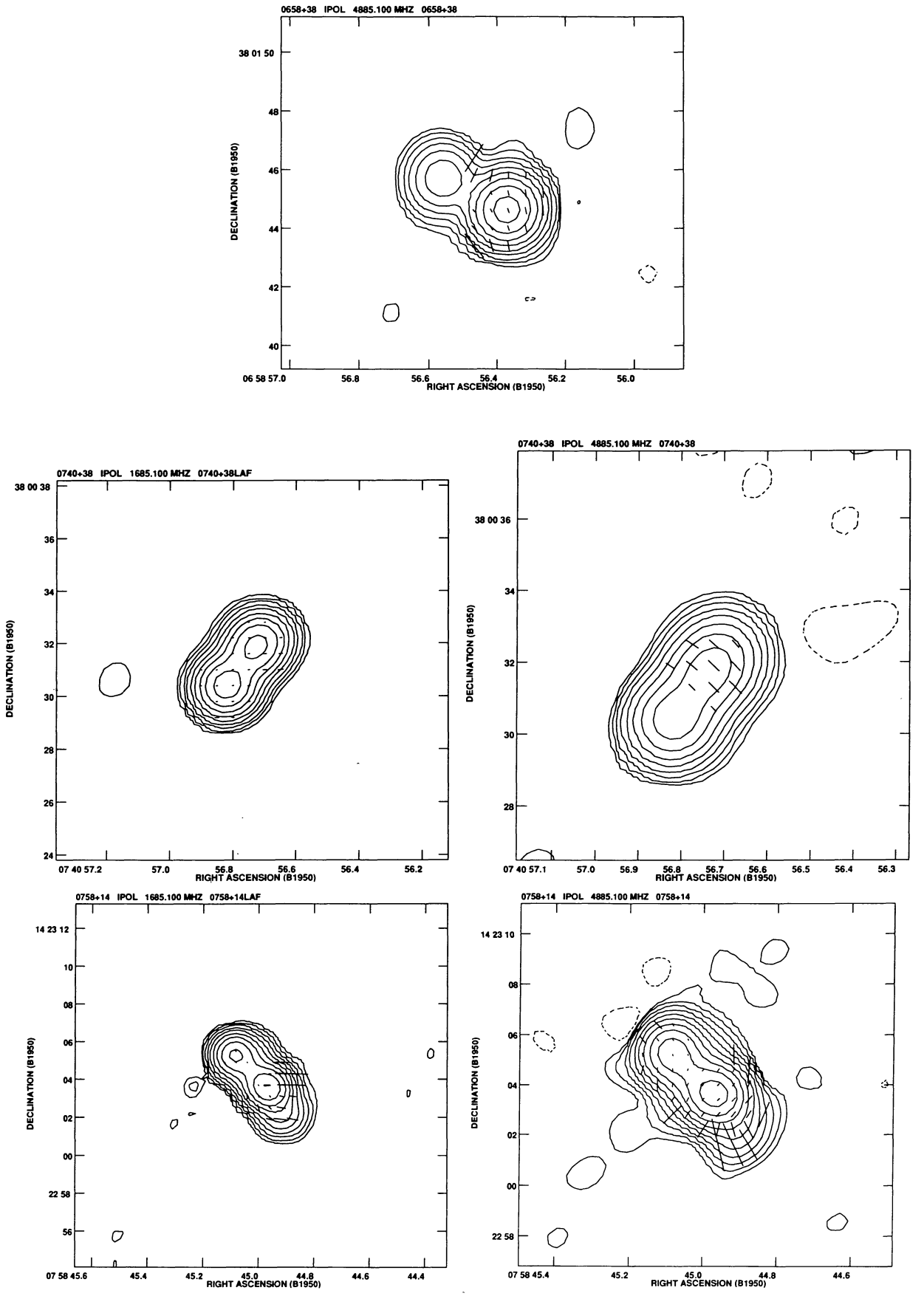


Fig. 4. continued

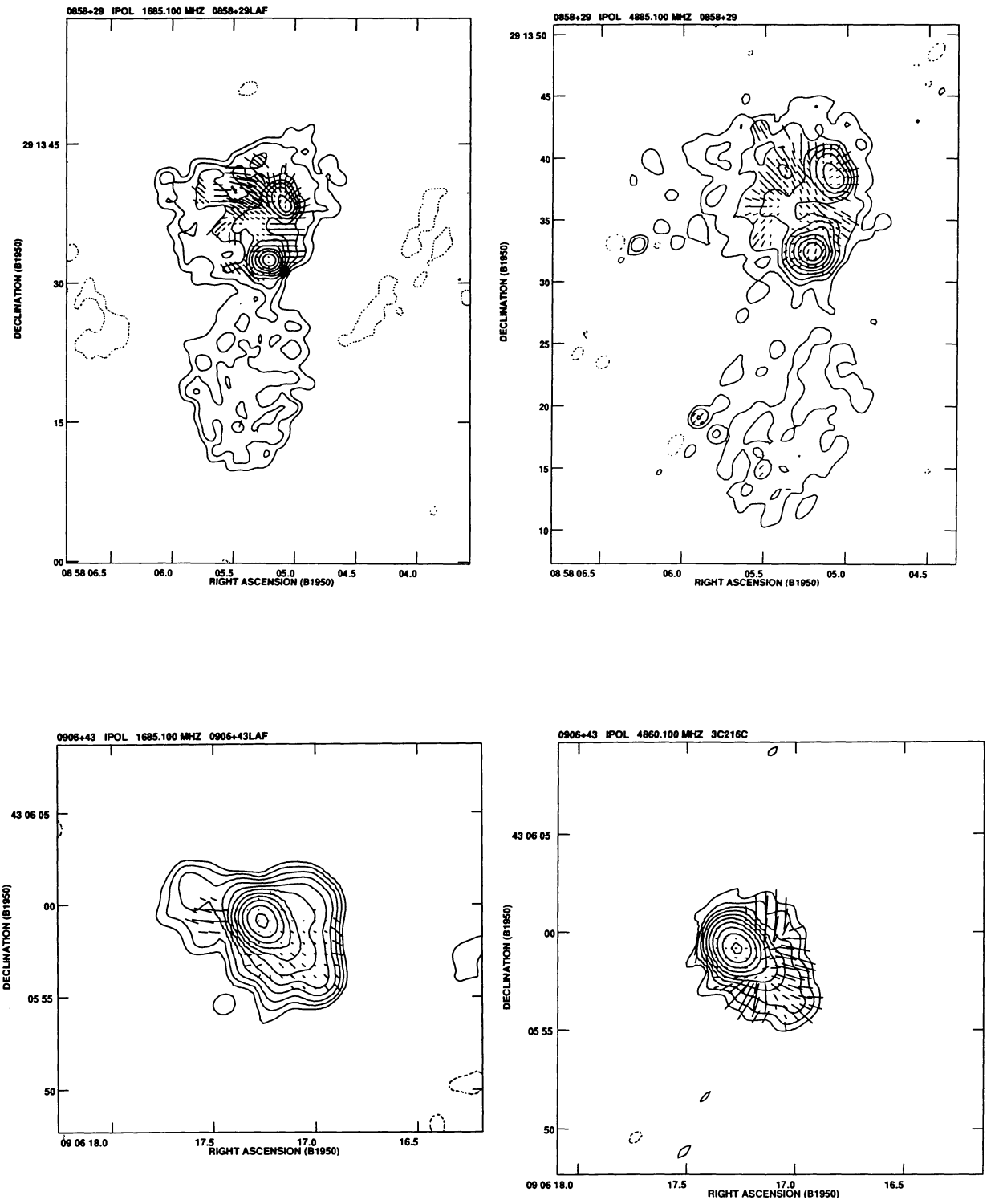


Fig. 4. continued

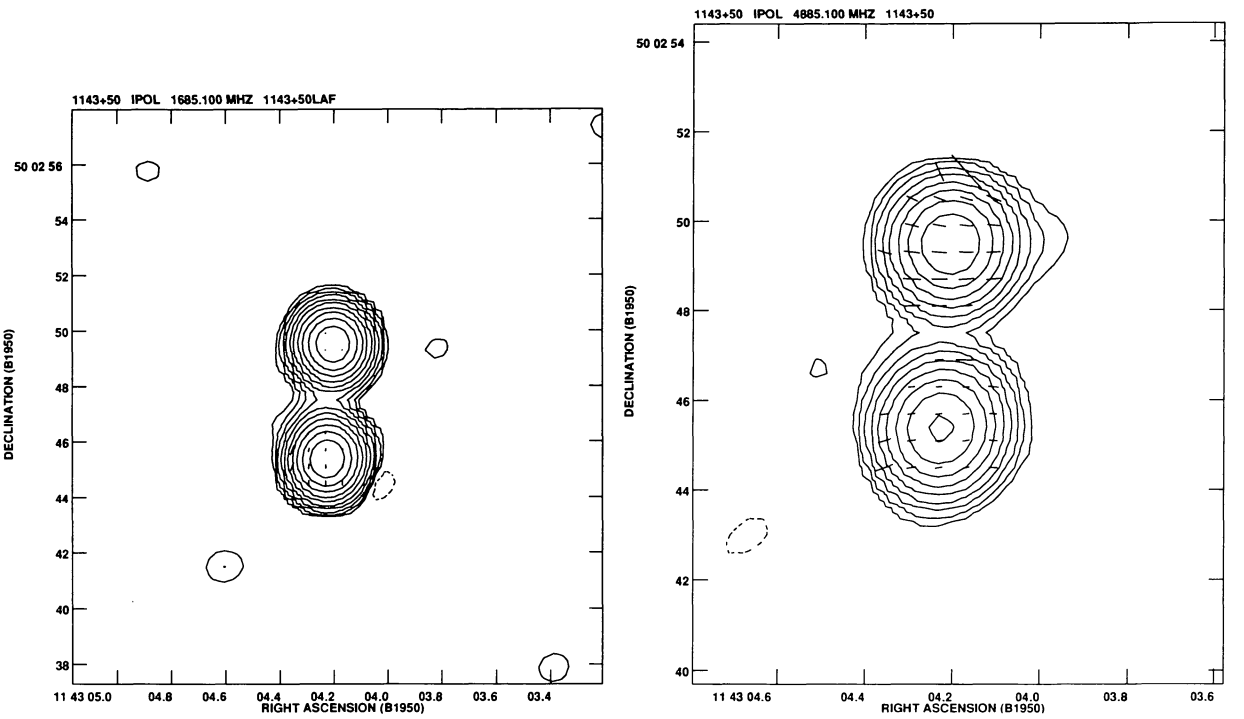


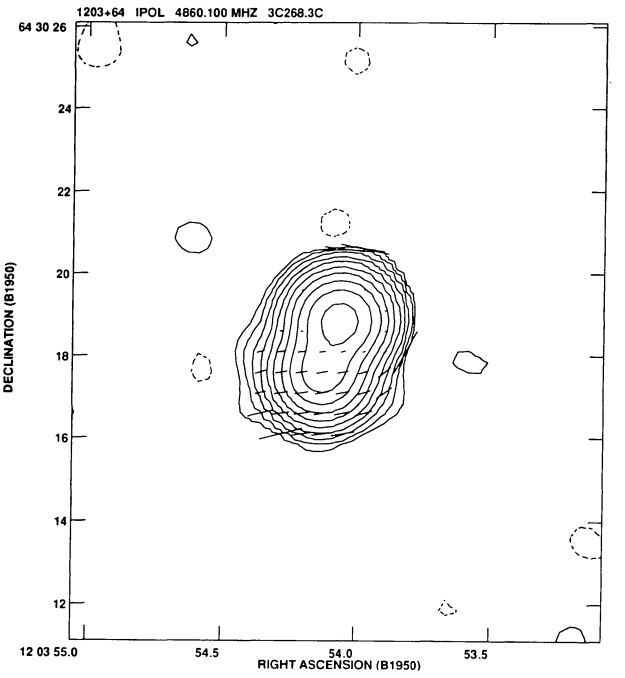


**Fig. 4.** continued

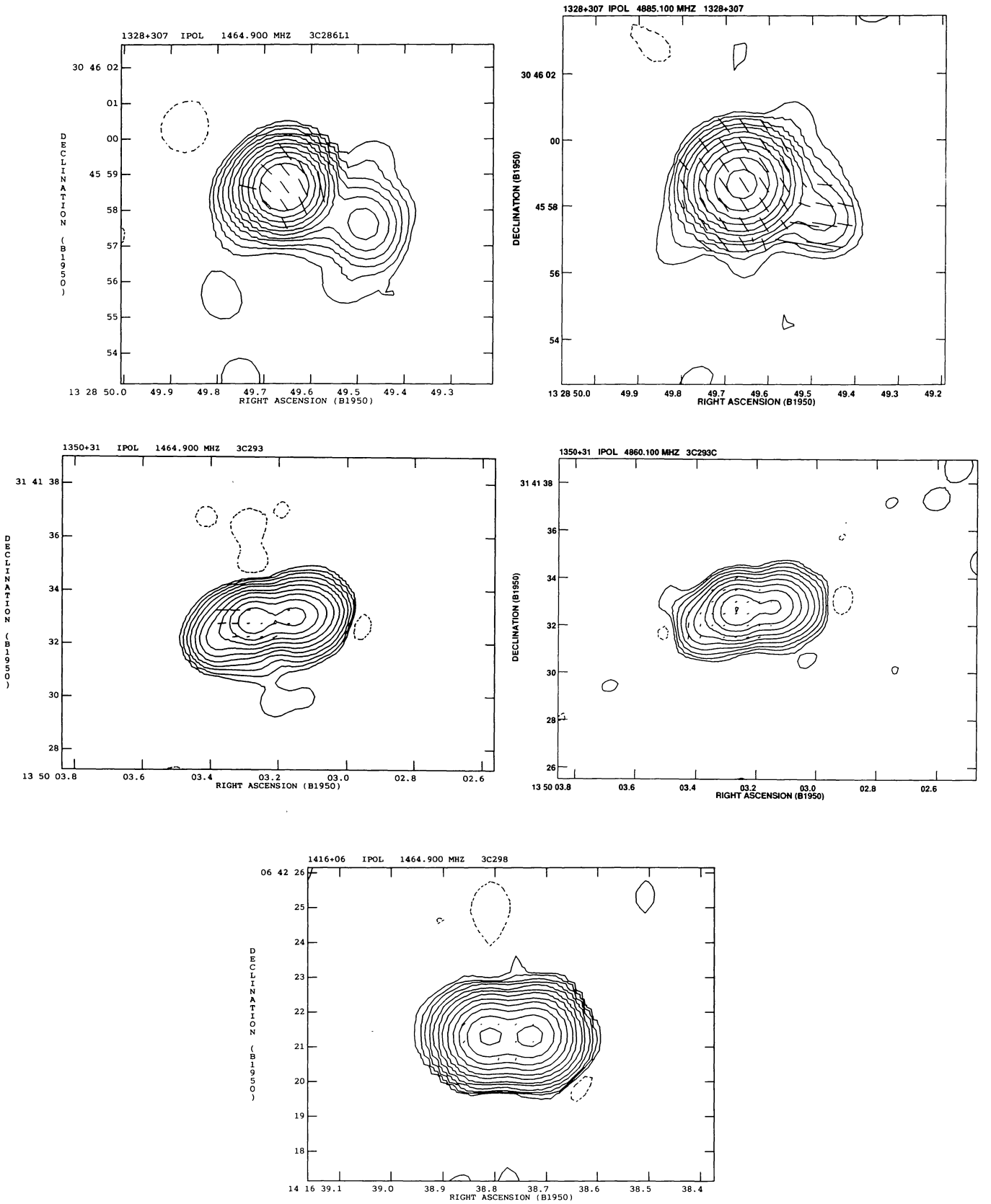


**Fig. 4.** continued

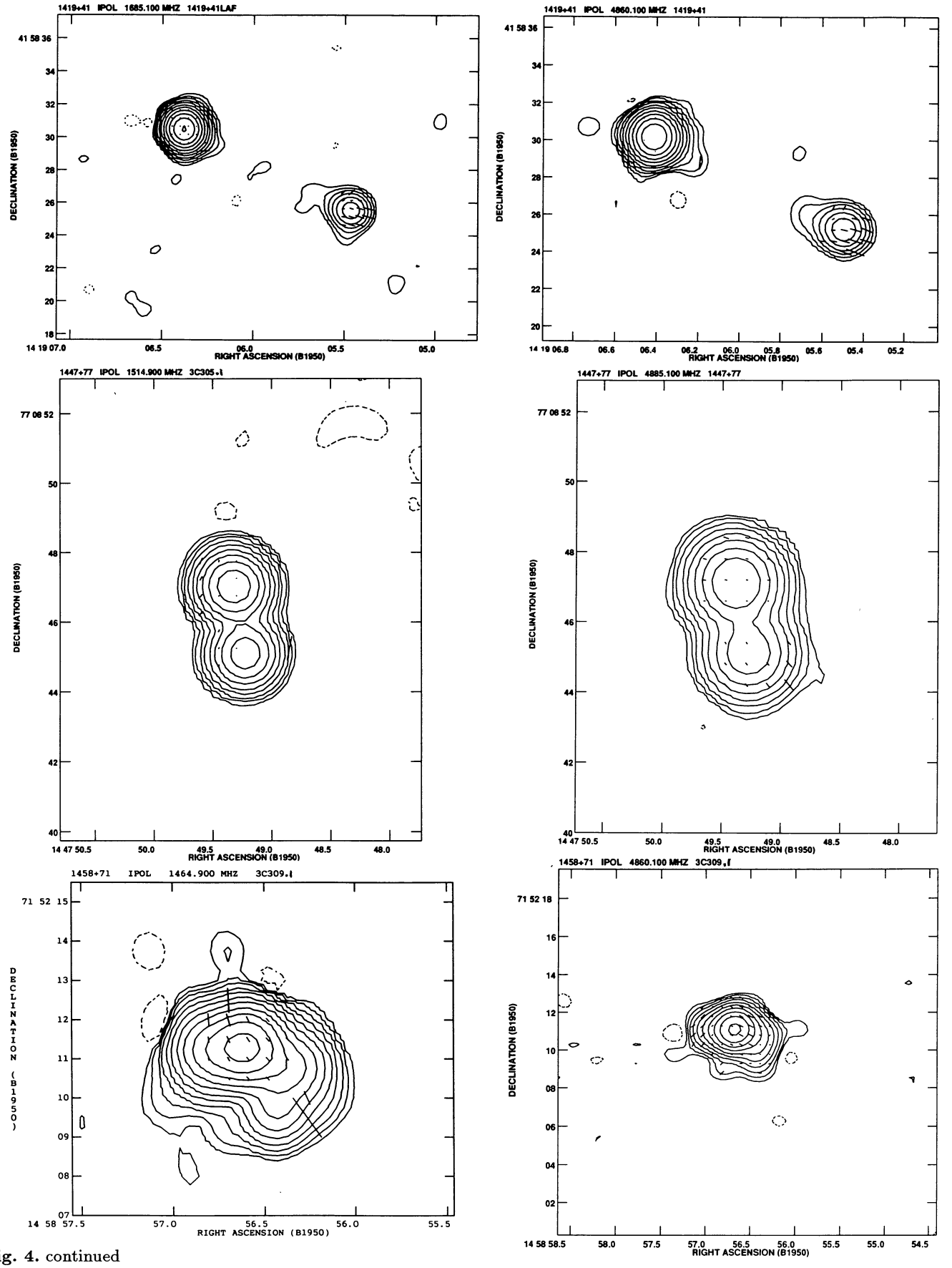


Fig. 4. continued

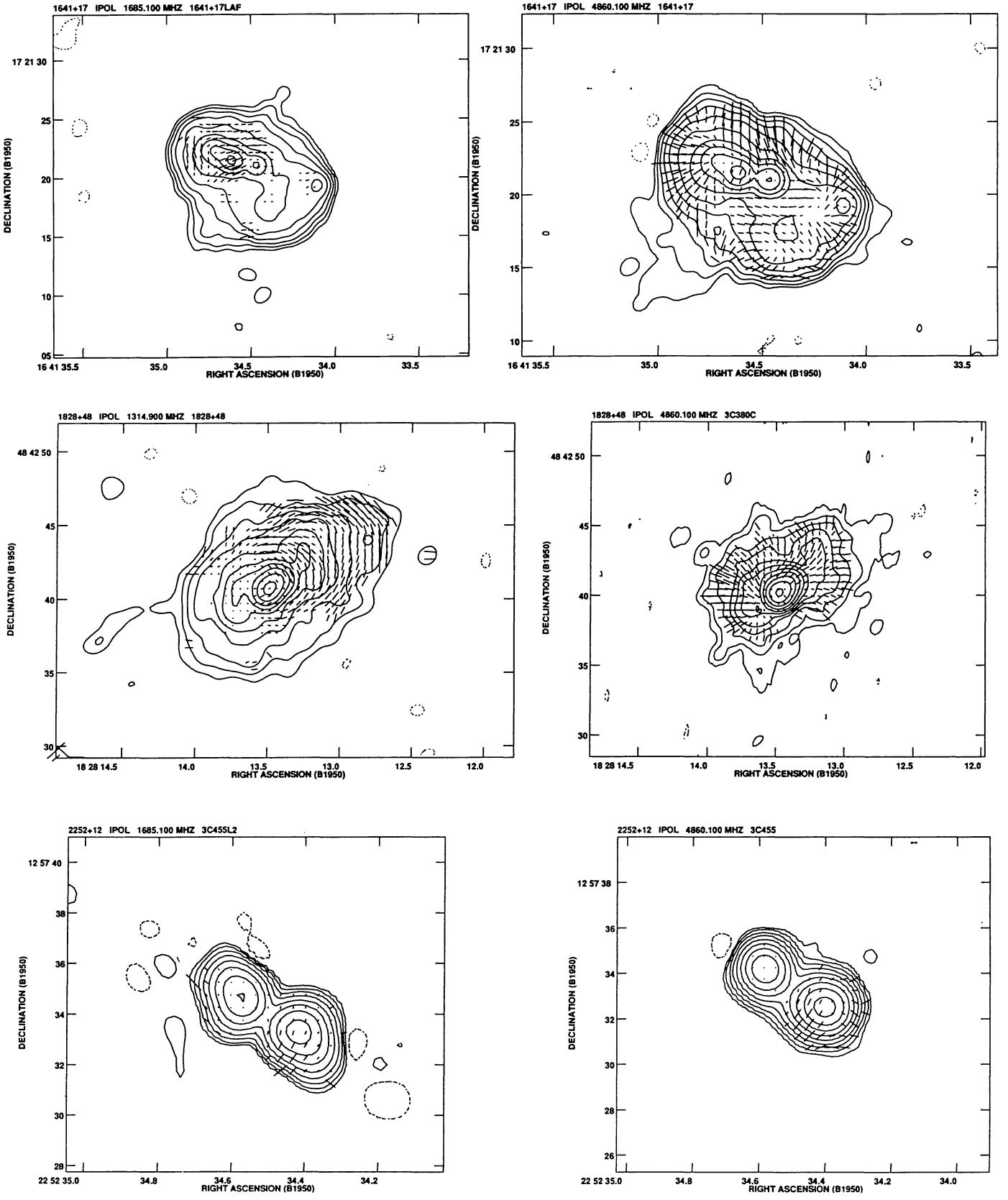


Fig. 4. continued

**Table 2.** Table of component polarization parameters measured from the maps at 8.4 GHz. $I$ and $P$ are the integrated component total and polarized intensity in mJy. The scalar and vector averaged percentage polarizations are $m_s$ and $m_v$ and the final column gives the error on the percentage polarization. The values for 3C49 and 3C295 are measured from data supplied by E. Ludke and G. Taylor respectively

| Source | Comp. | $I$ | $P$ | $m_s$ | $m_v$ | $\sigma_m$ |
|---|---|---|---|---|---|---|
| 3C43 | N | 16.0 | 1.3 | 8.1 | 8.7 | 0.8 |
| | E | 62.1 | 6.9 | 11.1 | 10.1 | 0.3 |
| | S | 611.7 | 23.5 | 3.8 | 2.6 | 0.3 |
| 3C48 | T | 2954.1 | 157.0 | 6.0 | 5.2 | 0.3 |
| 3C49 | E | 49.1 | 2.0 | < 5.0 | <5.0 | 1.7 |
| | W | 377.0 | 7.5 | 1.9 | 1.3 | 0.3 |
| 3C67 | N | 230.4 | 19.2 | 8.3 | 7.8 | 0.3 |
| | S | 354.0 | 0.9 | <0.3 | <0.3 | 0.3 |
| 3C93.1 | T | 480.9 | 6.1 | 1.3 | 1.1 | 0.3 |
| 3C138 | E | 2057.5 | 283.9 | 13.0 | 12.9 | 0.3 |
| | W | 514.3 | 44.2 | 2.0 | 2.0 | 0.3 |
| 3C147 | N | 517.0 | 18.9 | 3.7 | 4.3 | 0.3 |
| | S | 4615.0 | 131.1 | 2.8 | 2.9 | 0.3 |
| 3C173 | W | 223.1 | 5.3 | 2.4 | 2.2 | 0.3 |
| | C | 3.8 | 0.0 | <21.3 | <21.3 | 7.1 |
| | E | 31.4 | 0.7 | <2.6 | <2.6 | 0.9 |
| 3C186 | E1 | 41.0 | 0.0 | <1.8 | <1.8 | 0.6 |
| | E2 | 25.9 | 0.5 | <2.8 | <2.8 | 0.9 |
| | W1 | 22.7 | 0.3 | <3.2 | <3.2 | 1.1 |
| | W2 | 19.1 | 0.3 | <3.8 | <3.8 | 1.3 |
| 3C190 | N | 104.1 | 0.3 | <0.6 | 1.0 | 0.3 |
| | C | 67.2 | 0.4 | <0.9 | 1.0 | 0.3 |
| | S1 | 113.6 | 1.8 | 1.6 | 1.5 | 0.3 |
| | S2 | 134.0 | 0.2 | <0.5 | 0.6 | 0.3 |
| | S3 | 8.0 | 0.8 | 10.0 | <7.9 | 2.6 |
| 3C191 | N | 66.8 | 0.8 | 1.2 | <0.5 | 0.3 |
| | C | 34.8 | 0.4 | 1.1 | 1.0 | 0.3 |
| | J | 158.3 | 17.6 | 11.1 | 9.4 | 0.3 |
| 3C213.1 | N | 36.1 | 7.0 | 19.4 | 8.3 | 0.7 |
| | C | 13.5 | 0.2 | <5.3 | <5.3 | 1.8 |
| | S | 175.0 | 37.7 | 21.5 | 18.6 | 0.3 |
| 3C216 | N | 204.8 | 6.7 | 3.3 | 2.3 | 0.3 |
| | C | 886.6 | 14.1 | 1.6 | 0.9 | 0.3 |
| | S1 | 27.9 | 5.4 | 19.4 | 19.3 | 0.5 |
| | S2 | 2.1 | 0.0 | <21.4 | <21.4 | 7.1 |
| 3C237 | W | 642.3 | 6.4 | 1.0 | 1.0 | 0.3 |
| | E | 388.7 | 1.1 | <0.3 | <0.3 | 0.3 |
| 3C241 | W | 123.9 | 0.3 | <0.6 | <0.6 | 0.3 |
| | E | 43.1 | 0.2 | <1.7 | <1.7 | 0.6 |
| 3C266 | N | 77.1 | 3.6 | 4.7 | 3.3 | 0.3 |
| | S | 58.1 | 4.0 | 6.9 | 5.9 | 0.4 |
| 3C268.3 | N | 378.4 | 1.5 | 0.4 | 0.4 | 0.3 |
| | S | 237.5 | 20.1 | 8.5 | 8.1 | 0.3 |
| 3C277.1 | S | 255.4 | 1.9 | 0.7 | 0.8 | 0.3 |
| | C | 55.6 | 0.4 | <1.0 | <1.0 | 0.3 |
| | N | 159.6 | 13.6 | 8.5 | 8.4 | 0.3 |
| 3C286 | W1 | 31.4 | 6.7 | 21.3 | 14.7 | 3.3 |
| | W2 | 8.6 | 1.4 | <36.6 | <36.6 | 12.2 |
| | W3 | 16.9 | 2.3 | <18.6 | <18.6 | 6.2 |
| | C | 5208.5 | 597.6 | 11.5 | 11.4 | 0.3 |
| | E | 15.6 | 0.8 | <20.2 | <20.2 | 6.7 |
| 3C293 | W | 302.8 | 0.1 | <0.3 | < 0.3 | 0.3 |
| | E | 640.3 | 49.2 | 7.7 | 0.4 | 0.3 |
| 3C295 | N | 1448.0 | 28.0 | 1.9 | 1.2 | 0.1 |
| | S | 1743.3 | 81.2 | 4.7 | 1.4 | 0.1 |
| 3C298 | W1 | 163.8 | 0.1 | <0.4 | <0.4 | 0.3 |
| | W2 | 427.9 | 0.7 | <0.3 | <0.3 | 0.3 |
| | E1 | 283.5 | 24.0 | 8.5 | 5.9 | 0.3 |
| 3C299 | W | 20.1 | 5.0 | 24.9 | 16.0 | 1.0 |
| | E | 441.6 | 13.1 | 3.0 | 1.1 | 0.3 |
| 3C303.1 | N | 17.9 | 0.2 | <3.5 | <3.5 | 1.2 |
| | S | 176.3 | 2.0 | 1.1 | 1.1 | 0.3 |
| 3C305.1 | S | 22.1 | 1.6 | 7.2 | 7.9 | 1.4 |
| | N2 | 58.6 | 2.0 | 3.4 | 2.3 | 0.5 |
| | N1 | 43.4 | 1.9 | 4.3 | 3.4 | 0.7 |
| 3C309.1 | W | 122.9 | 4.7 | 3.8 | 1.2 | 0.3 |
| | C | 1574.5 | 87.5 | 5.6 | 5.2 | 0.3 |
| | E | 388.7 | 31.7 | 8.2 | 4.4 | 0.3 |
| 3C318 | S | 84.8 | 0.6 | <1.4 | <1.4 | 0.5 |
| | N | 280.0 | 30.1 | 10.8 | 10.8 | 0.3 |
| 3C343.1 | T | 667.3 | 0.1 | <0.3 | <0.3 | 0.3 |
| 3C346 | C | 221.0 | 0.1 | <0.3 | 0.4 | 0.3 |
| | E | 103.5 | 17.3 | 16.7 | 16.0 | 0.3 |
| 3C380 | E | 200.6 | 43.0 | 21.4 | 7.9 | 0.3 |
| | C | 2853.8 | 124.6 | 4.2 | 4.4 | 0.3 |
| | W | 814.6 | 86.4 | 10.6 | 9.1 | 0.3 |
| 3C454.1 | N | 84.6 | 2.5 | 3.0 | 2.6 | 0.3 |
| | S | 33.5 | 0.8 | 2.4 | <2.1 | 0.7 |
| 3C455 | W | 227.4 | 29.5 | 13.0 | 3.3 | 0.3 |
| | E | 120.2 | 2.3 | 1.9 | 1.2 | 0.3 |

galaxy with a total extent of about 35 kpc across and should not really be classed as a CSS source. Liu and Pooley (1991) also find strong depolarization at 20 cm in the northern component and suggest that this is caused by line emitting gas to the north-east of the core (McCarthy et al. 1991).

**3C303.1 (1443+77)**

This source is very asymmetric in brightness and polarization at 8.4 GHz.

**3C309.1 (1458+71)**

The jet to the east is highly polarized, whereas the lobe on the opposite side only shows significant polarization along its outer edge.

**3C318 (1517+20)**

This source shows strong polarization asymmetry at 8.4 GHz: the northern polarized component consists of a knotty jet at high resolution (Spencer et al. 1991).

**3C343.1 (1637+62)**

This compact source is unpolarized at both 8.4 and 15 GHz.

**3C346 (1641+17)**

The jet to the east is highly polarized. Lower resolution maps reveal a cocoon (Pooley & Henbest 1974; Spencer et al. 1991) which shows strong depolarization on the western side between 6 and 20 cm (see Akujor et al., in prep.).

**3C380 (1828+48)**

This source has been discussed in detail by Wilkinson et al. (1990). We confirm the very asymmetric depolarization between 1.3 and 5 GHz.

**3C454.1 (2248+71)**

This source is quite symmetric in brightness and polarization.

**3C455 (2252+12))**

The diffuse western lobe is highly polarized. More sensitive observations are needed to see whether the slight extension on the eastern side of this lobe is the nucleus.

## 5. Conclusions

The interpretation of the polarization results is presented in another paper, but the main results of our investigation are as follows:

1. Our high resolution 8.4 GHz maps which are more sensitive than previous 5 and 15 GHz VLA maps, but have intermediate resolution, confirm the structures seen in previous maps and reveal various new features. For example, we have found nuclear components in 3C173, 3C213.1 and 3C293.
2. In most cases where the cores were detected, the brighter component is nearer to the core. This is true for quasars and radio galaxies. In quasars, the jet tends to point to the brighter component. In radio galaxies, it appears that the brighter component nearer to the core is also more compact, but higher resolution data are required to confirm this.

**Table 2.** Table of total intensity,fractional polarizations and spectral index ($S \propto \nu^{-\alpha}$) for the scaled-array observations at 1.6 and 4.9 GHz

| Source | Comp. | 4.9 GHz | | 1.6 GHz | | $\alpha$ |
|---|---|---|---|---|---|---|
| | | $I$/mJy | $m_v$/% | $I$/mJy | $m_v$/% | |
| 3C43 | T | 1078.0 | 3.0 | | | |
| | N | 60.8 | 18.2 | | | |
| | S | 1018.0 | 3.0 | | | |
| 3C67 | T | 1009.9 | 1.7 | 2713.0 | 1.4 | 0.85 |
| | N | 373.8 | 4.6 | 1103.8 | 2.2 | 0.93 |
| | S | 638.0 | <0.3 | 1612.6 | 1.4 | 0.79 |
| 3C173 | T | 442.1 | 0.4 | | | |
| | N | 74.4 | 0.5 | | | |
| | S | 373.0 | 0.6 | | | |
| 3C186 | T | 240.6 | 1.1 | 845.4 | 0.6 | 1.19 |
| | N | 113.6 | 1.1 | 378.0 | 0.7 | 1.14 |
| | S | 127.2 | <0.3 | 467.0 | 0.6 | 1.23 |
| 3C190 | T | 760.6 | 0.4 | 1702.9 | 0.6 | 0.76 |
| | N | 290.0 | 0.3 | 628.7 | 0.9 | 0.73 |
| | S | 470.0 | 0.5 | 1074.0 | 0.8 | 0.78 |
| 3C213.1 | T | 817.6 | 4.9 | 1874.7 | 1.5 | 0.78 |
| | N | 257.2 | 7.5 | 604.7 | 5.1 | 0.81 |
| | C | 460.0 | 7.6 | 961.7 | 2.1 | 0.70 |
| | S | 100.2 | 8.6 | 304.0 | 4.7 | 1.05 |
| 3C216 | T | 1576.2 | 2.0 | 3393.7 | 0.9 | 0.73 |
| | C | 1467.5 | 2.1 | 2980.7 | 1.0 | 0.67 |
| 3C266 | T | 303.3 | 3.7 | 1161.7 | 0.5 | 1.27 |
| | N | 137.1 | 4.8 | 564.3 | 0.3 | 1.34 |
| | S | 166.1 | 2.7 | 596.5 | 0.9 | 1.21 |
| 3C268.3 | T | 1159.9 | 2.1 | | | |
| | N | 641.9 | <0.3 | | | |
| | S | 516.0 | 4.2 | | | |
| 3C286 | T | 7584.0 | 11.0 | 13697.0 | 9.8 | 0.56 |
| | C | 7522.7 | 11.1 | 13424.0 | 10.0 | 0.55 |
| | SW | 96.2 | 13.1 | 271.2 | 7.1 | 0.98 |
| 3C293 | T | 1548.7 | 0.8 | 3741.6 | <0.3 | 0.83 |
| | E | 1005.3 | 1.0 | 2132.7 | 0.3 | 0.71 |
| | W | 542.8 | 0.3 | 1612.8 | 0.5 | 1.03 |
| 3C298 | T | | | 5404.5 | 0.5 | |
| | E | | | 2685.0 | 0.5 | |
| | W | | | 2693.8 | 0.5 | |
| 3C299 | T | | | | | |
| | N | 852.5 | <0.3 | 2402.6 | 0.5 | 0.98 |
| | S | 51.0 | 7.0 | 119.7 | 6.2 | 0.81 |
| 3C305.1 | T | 406.6 | 0.7 | 1433.2 | 0.3 | 1.07 |
| | N | 284.2 | 0.9 | 980.0 | 0.3 | 1.06 |
| | S | 122.3 | 1.3 | 451.4 | 0.5 | 1.11 |
| 3C309.1 | T | 3110.0 | 2.8 | 6748.6 | 1.8 | 0.65 |
| 3C346 | T | 1483.0 | 1.0 | 3179.9 | 2.8 | 0.72 |
| | E | 1021.2 | 2.0 | 2131.2 | 3.2 | 0.70 |
| | W | 459.2 | 2.3 | 1050.6 | 1.3 | 0.78 |
| 3C380 | T | 6317.9 | 1.9 | 12012.8 | 0.9 | 0.61 |
| | E | 3023.6 | 3.9 | 6416.8 | 1.3 | 0.71 |
| | W | 3274.9 | 4.3 | 5586.8 | 2.9 | 0.51 |
| 3C455 | T | 766.1 | 2.3 | 2270.4 | 1.9 | 1.03 |
| | N | 282.8 | 0.3 | 981.4 | 0.8 | 1.18 |
| | S | 482.8 | 3.6 | 1286.7 | 3.4 | 0.93 |

**Table 3.** Table of component polarization values measured from the maps at 15 GHz. Columns are as for Table 2

| Source | Comp. | $I$ | $m_s$ | $m_v$ | $\sigma_m$ |
|---|---|---|---|---|---|
| 3C48 | T | 1542 | 8.2 | 6.5 | 0.3 |
| | S | 498 | 6.3 | 5.0 | 0.3 |
| | N | 1035 | 8.8 | 8.0 | 0.3 |
| 3C138 | T | 1467 | 13.3 | 11.8 | 0.3 |
| | W | 52 | < 10.3 | < 10.3 | 3.4 |
| | C | 267 | 7.2 | 4.9 | 0.7 |
| | E | 1171 | 14.9 | 14.1 | 0.2 |
| 3C147 | S | 2665 | 2.9 | 2.5 | 0.3 |
| | N | 176 | 13.2 | 12.4 | 1.0 |
| 3C173 | S | 6 | < 44.0 | 49.4 | 14.7 |
| | N | 98 | 6.7 | < 2.8 | 0.9 |
| 3C186 | C | 33 | < 3.5 | < 3.5 | 1.2 |
| 3C268.3 | S | 65 | 11.6 | 10.5 | 1.9 |
| | N | 118 | < 3.1 | < 3.1 | 1.0 |
| 3C277.1 | T | 269 | 12.9 | 2.1 | 0.4 |
| | N | 75 | 11.0 | 10.6 | 1.6 |
| | C | 51 | < 7.0 | < 7.0 | 2.3 |
| | S | 134 | 3.4 | 3.3 | 0.9 |
| 3C293 | T | 520 | 19.4 | 6.6 | 0.3 |
| | E | 330 | 15.9 | 10.8 | 0.3 |
| | W | 162 | 2.6 | 0.5 | 0.3 |
| 3C309.1 | T | 1479 | 10.5 | 3.1 | 0.3 |
| | W | 40 | 75.7 | < 11.2 | 3.7 |
| | C | 1282 | 4.7 | 4.0 | 0.3 |
| | J | 26 | 19.0 | 17.2 | 5.7 |
| | E | 130 | 11.4 | 4.4 | 1.2 |
| 3C343.1 | T | 315 | < 1.4 | < 1.4 | 0.5 |
| | W | 211 | < 2.1 | < 2.1 | 0.7 |
| | E | 104 | < 4.2 | < 4.2 | 1.4 |

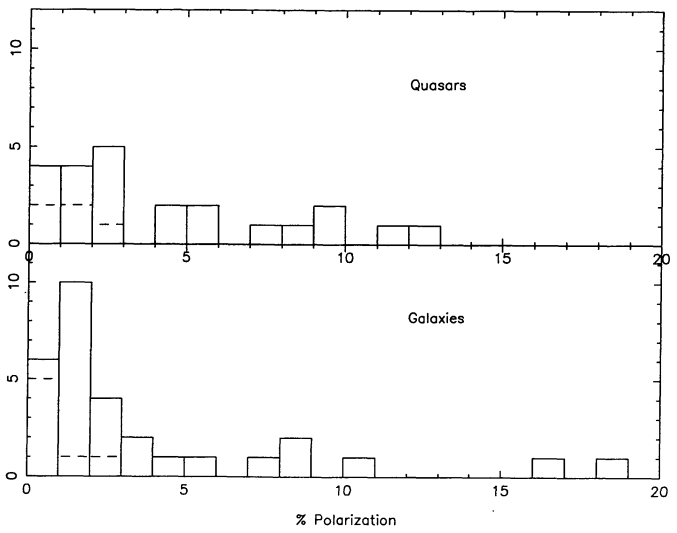


**Fig. 5.** Histogram of the fractional polarization of the CSS components at 8.4 GHz. In quasars with several subcomponents only the brightest subcomponent on each side of the nucleus has been used. Weak components where the fractional polarization could not be determined to better than 5% and flat-spectrum nuclear components have also been omitted. Upper limits are indicated by a dashed line

**Table 4.** Contour levels and polarization scale for the 8.4 and 15 GHz maps. Contours are plotted at equal logarithmic intervals of ×2 above the lowest contour

| Source | Lowest contour mJy/beam | Peak mJy/beam | Pol. scale %/arcsec |
|---|---|---|---|
| | 8.4 GHz | | |
| 3C48 | 5 | 1589.5 | 89 |
| 3C43 | 1 | 450.4 | 100 |
| 3C67 | 0.75 | 256.4 | 80 |
| 3C93.1 | 1 | 301.5 | 89 |
| 3C138 | 2 | 1578.8 | 167 |
| 3C147 | 5 | 3464.8 | 100 |
| 3C173 | 0.25 | 201.7 | 50 |
| 3C186 | 0.25 | 301.5 | 89 |
| 3C190 | 0.25 | 84.7 | 57 |
| 3C191 | 0.25 | 41.9 | 133 |
| 3C213.1 | 0.25 | 83.7 | 80 |
| 3C216 | 0.25 | 755.2 | 40 |
| 3C237 | 0.25 | 522.4 | 20 |
| 3C241 | 0.25 | 96.2 | 67 |
| 3C268.3 | 0.25 | 314.1 | 100 |
| 3C277.1 | 0.25 | 211.1 | 83 |
| 3C286 | 0.5 | 5089.4 | 133 |
| 3C293 | 0.5 | 204.2 | 100 |
| 3C298 | 0.5 | 290.2 | 83 |
| 3C299 | 0.5 | 147.8 | 83 |
| 3C303.1 | 0.25 | 133.8 | 167 |
| 3C305.1 | 0.25 | 70.06 | 100 |
| 3C309.1 | 0.5 | 1442.6 | 83 |
| 3C318 | 2 | 265.6 | 100 |
| 3C343.1 | 1 | 445.15 | 13 |
| 3C346 | 0.25 | 207.0 | 80 |
| 3C380 | 1.0 | 2853.8 | 167 |
| 3C454.1 | 0.25 | 71.78 | 20 |
| 3C455 | 0.25 | 46.72 | 111 |
| | 15 GHz | | |
| 3c48 | 5 | 545.4 | 267 |
| 3C138 | 2 | 712.8 | 267 |
| 3C147 | 2.5 | 1657.4 | 267 |
| 3C173 | 0.75 | 56.93 | 200 |
| 3C268.3 | 3 | 68.84 | 267 |
| 3C277.1 | 1.0 | 106.7 | 160 |
| 3C293 | 1.0 | 85.4 | 267 |
| 3C309.1 | 1.0 | 1177.9 | 267 |
| 3C343.1 | 1.0 | 181.0 | - |

3. The degree of polarization of the components at 8.4 GHz is generally low (median value 3%). Several quasars have significantly higher than average polarization (see Fig. 5), but part of this effect is due to the presence of more highly polarized jets in these sources. Statistical tests which take into account the upper limits to the polarization do not show any significant difference between the radio galaxies and quasars, but the number of upper limits make these tests rather weak.
4. Many sources show a striking asymmetry in the component polarization at 8.4 GHz. In general it is the

**Table 5.** Contour levels and polarization scales for the 1.5 and 4.9 GHz maps (Fig. 4)

| Source | 1.6 GHz | | | 5 GHz | | |
|---|---|---|---|---|---|---|
| | Lowest contour | Peak | Pol. scale | Lowest contour | Peak | Pol. scale |
| 3C43 | | | | 0.75 | 864.7 | 267 |
| 3C67 | 1.0 | 1621.0 | 20 | 0.5 | 582.1 | 20 |
| 3C173 | | | | 1.0 | 356.7 | 3.3 |
| 3C186 | 1.0 | 397.5 | 6.7 | 0.5 | 106.5 | 3.3 |
| 3C190 | 1.5 | 776.2 | 6.7 | 0.5 | 372.7 | 3.3 |
| 3C213.1 | 1.0 | 487.1 | 22 | 0.5 | 250.6 | 33 |
| 3C216 | 1.5 | 1813.7 | 22.0 | 2.0 | 1164.7 | 26.7 |
| 3C266 | 0.5 | 501.1 | 6.7 | 0.5 | 146.1 | 16.7 |
| 3C268.3 | | | | 1.0 | 724.8 | 20.0 |
| 3C286 | 4.0 | 13528.0 | 20.0 | 5.0 | 7092.6 | 22.0 |
| 3C293 | 1.5 | 1334.5 | 8.0 | 1.5 | 779.5 | 13.3 |
| 3C298 | 1.0 | 2571.5 | 8.0 | | | |
| 3C299 | 2.0 | 2160.7 | 26.7 | 0.75 | 762.6 | 22.0 |
| 3C305.1 | 2.0 | 888.1 | 16.0 | 1.0 | 265.1 | 16.7 |
| 3C309.1 | 3.0 | 4428.5 | 20.0 | 4.0 | 2422.9 | 20.0 |
| 3C346 | 1.5 | 454.8 | 13.0 | 1.0 | 262.6 | 22.0 |
| 3C380 | 7.5 | 4896.0 | 20.0 | 3.0 | 3456.9 | 26.7 |
| 3C455 | 5.0 | 900.7 | 26.7 | 1.0 | 353.5 | 26.7 |

jet sides of quasars and the components further from the core in radio galaxies which have higher degrees of polarization.

5. The degree of polarization is higher at 15 GHz (median value 6%), which is consistent with the value of 7% found by van Breugel (1992).
6. The degree of polarization is very low at 4.9 GHz (median value about 2%) and lower still at 1.6 GHz (median less than 1%).
7. A few sources (3C93.1, 3C241, 3C343.1) are unpolarized at all frequencies.

*Acknowledgements.* We are grateful to the VLA staff, especially Barry Clark, Peggy Perley and Dave Wunker for repeating observations affected by power failure. CEA acknowledges Swedish NFR fellowship at Onsala and thanks Prof. R.S. Booth, Prof. R.D. Davies and Dr. Ian Browne for encouragement. STG thanks Prof. R.S. Booth for hospitality during a visit to Onsala in connection with this project. NRAO-VLA is operated by Associated Universities Inc. under contract with the US National Science Foundation

## References

Akujor C.E., Spencer R.E., Saikia D.J. 1991, A&A 249, 337
Akujor C.E., Spencer R.E., Zhang F.J. et al. 1993, A&A 274, 752
Baars J.W.M., Genzel R., Witzel A. 1977, A&AS 61, 99
Bridle A., Fomalont E., Cornwell T. 1981, AJ 86, 1294
Cawthorne T.V., Scheuer P.A.G., Morison I., Muxlow T.W.B. 1986, MNRAS 219, 883
Fejes I., Porcas R.W., Akujor C.E. 1992, A&A 257, 459
Fanti C., Fanti R., Parma P., Schilizzi R.T., van Breugel W.J.M. 1985, A&A 143, 292
Fanti R., Fanti C., Schilizzi R.T. et al. 1990, A&A 231, 333
Garrington S.T., Leahy J.P., Conway R.G., Laing R.A. 1988, Nature 331, 147
Garrington S.T., Conway R.G., Leahy J.P. 1991, MNRAS 250, 171
Kato T., Tabara H., Inoue M., Aizu K. 1987, Nature 329, 223
Kronberg P.P., Perry J.J., Zukowski E.L.H. 1990, ApJ 355, L31
Laing R.A., Riley J.M., Longair M.S. 1983, MNRAS 204, 151
Laing R.A. 1988, Nature 331, 149
Liu R., Pooley G. 1991, MNRAS 249, 343
McCarthy P.J., van Breugel W.J.M., Kapahi V.K. 1991, ApJ 371, 478
Orr M.J.L., Browne I.W.A. 1982, MNRAS 200, 1067
Pearson T.J., Perley R.A., Readhead A.C.S. 1985, AJ 90, 738
Pooley G.G., Henbest S.N. 1974, MNRAS 169, 477
Sanghera H.S. et al. 1994, A&A, in press
Spencer R.E., McDowell J.C., Charlesworth M. et al. 1989, MNRAS 240, 657
Spencer R.E., Schilizzi R.T., Fanti C. et al. 1991, MNRAS 250, 225
van Breugel W.J.M., Miley G., Heckman T. 1984, AJ 89, 5
van Breugel W.J.M, Fanti C., Fanti R. et al. 1992, A&A 256, 56
Wilkinson P.N., Akujor C.E., Cornwell T.J., Saikia D.J. 1990, MNRAS 248, 86